ELSEVIER

Contents lists available at ScienceDirect

International Journal of Biological Macromolecules

journal homepage: www.elsevier.com/locate/ijbiomac





Effects of ferritin iron loading, subunit composition, and the NCOA4-iron sulfur cluster on ferritin-NCOA4 interactions: An isothermal titration calorimetry study

Fadi Bou-Abdallah*, Mohamed Boumaiza, Ayush K. Srivastava

Department of Chemistry, State University of New York, Potsdam, NY 13676, USA

ARTICLE INFO

Keywords: Ferritinophagy Nuclear receptor coactivator-4 (NCOA4) Isothermal titration calorimetry (ITC)

ABSTRACT

Ferritin is a 24-mer protein nanocage that stores iron and regulates intracellular iron homeostasis. The nuclear receptor coactivator-4 (NCOA4) binds specifically to ferritin H subunits and facilitates the autophagic trafficking of ferritin to the lysosome for degradation and iron release. Using isothermal titration calorimetry (ITC), we studied the thermodynamics of the interactions between ferritin and the soluble fragment of NCOA4 (residues 383–522), focusing on the effects of the recently identified Fe—S cluster bound to NCOA4, ferritin subunit composition, and ferritin-iron loading. Our findings show that in the presence of the Fe—S cluster, the binding is driven by a more favorable enthalpy change and a decrease in entropy change, indicating a key role for the Fe—S cluster in the structural organization and stability of the complex. The ferritin iron core further enhances this association, increasing binding enthalpy and stabilizing the NCOA4-ferritin complex. The ferritin subunit composition primarily affects binding stoichiometry of the reaction based on the number of H subunits in the ferritin H/L oligomer. Our results demonstrate that both the Fe—S cluster and the ferritin iron core significantly affect the binding thermodynamics of the NCOA4-ferritin interactions, suggesting regulatory roles for the Fe—S cluster and ferritin iron content in ferritinophagy.

1. Introduction

Iron is essential for various biological processes but can be harmful in excess [1]. In mammals, iron levels are tightly regulated through coordinated mechanisms involving uptake, storage, release, export, and redistribution [2,3]. Several proteins and factors, such as the peptide hormone hepcidin [4], iron regulatory proteins IRP1 and IRP2 [5], hypoxia-inducible factor (HIF) [6,7], and the iron storage protein ferritin [8-13], play significant roles in maintaining iron balance. Eukaryotic ferritin is an oligomer composed of 24 subunits of two types, H (for Heavy, ~21 kDa) and L (for Light, ~19 kDa) that self-assemble into spherical nanocages of approximately 12 nm in outer diameter and 8 nm in inner diameter where thousands of iron atoms can be stored in the form of an inorganic iron core [8,9]. These protein nanocages have eight narrow 3-fold hydrophilic channels and six 4-fold hydrophobic channels, each about 4 Å in diameter. The 3-fold channels are the main pathways through which Fe^{2+} cations reach the catalytic ferroxidase centers on the H subunits where it gets oxidized before it moves to the inner ferritin cavity for deposition and iron core formation [8].

While the H subunit is responsible for the rapid oxidation of Fe^{2+} to Fe^{3+} at its dinuclear ferroxidase centers, L subunit aids in iron nucleation and mineralization. In mammals, the H and L subunits co-assemble in varying ratios depending on cell type and physiological state. For instance, ferritins rich in H subunits are typically found in tissues with high metabolic rates, such as the heart, kidney, and brain, while those rich in L subunits are found in tissues with iron storage functions, such as the liver and spleen [14].

Recent research highlighted the dynamic nature of ferritin beyond passive iron storage, but its fate and iron content within the cytosol remain unclear [15,16]. It has been shown that ferritin undergoes degradation through either the proteasome or a combination of lysosomal and proteasomal pathways. Under iron-depleted conditions, ferritin is transported to lysosomes for degradation and iron recycling via ferritinophagy, facilitated by the autophagy receptor NCOA4, which binds exclusively to H-ferritin [17,18]. Under iron-replete conditions, NCOA4 interacts with HERC2, leading to its degradation by the proteasome, thereby inhibiting ferritinophagy and promoting ferritin accumulation [18–21]. A recent study found that NCOA4 contains an

E-mail address: bouabdf@potsdam.edu (F. Bou-Abdallah).

^{*} Corresponding author.

Table 1 Experimentally determined ITC conditional binding parameters for the titrations of apo-NCOA4-D (lacking a Fe—S cluster), holo-NCOA4-D (containing a Fe—S cluster) with different types of ferritins (apo and holo, homopolymers and heteropolymers). Conditions are those reported in Figs. 2, 3 and 4. The reported thermodynamic quantities (i.e. binding stoichiometry n, binding affinity Ka, enthalpy change ΔH, entropy change ΔS, and free energy change ΔG) are apparent average values with standard deviation from replicate measurements ($2 \le N \le 3$).

${\bf Holo\text{-}NCOA4\text{-}D} + {\bf Apo\text{-}Ferritin}$	n	ΔH (kJ/mol)	$\Delta S (J/mol \cdot K)^a$	ΔG (kJ/mol) ^b	$K_a \times 10^{-6} (M^{-1})$
Apo-FtH [24H:0L]	2.4 ± 0.21	-49.9 ± 0.88	-58.6 ± 0.68	-32.4 ± 0.85	2.1 ± 0.64
Apo-[21H:3L]	2.5 ± 0.53	-46.4 ± 1.35	-51.3 ± 2.42	-31.1 ± 1.34	3.5 ± 0.84
Apo-[12H:12L]	1.6 ± 0.22	-48.7 ± 1.07	-44.1 ± 3.74	-35.6 ± 1.05	0.7 ± 0.54
Average		-48.4 ± 1.36	-51.3 ± 7.25	-33.1 ± 2.31	2.1 ± 1.4
Holo-NCOA4-D + Holo-Ferritin (~500 Fe ^{III} /shell)	n	ΔH (kJ/mol)	ΔS (J/mol·K) ^a	ΔG (kJ/mol) ^b	$K_a \times 10^{-6} (M^{-1})$
Holo-FtH [24H:0L]	4.7 ± 0.91	-56.8 ± 5.92	-77.6 ± 9.36	-33.7 ± 5.94	1.3 ± 0.27
Holo-[21H:3L]	5.8 ± 0.15	-54.9 ± 1.85	-77.0 ± 9.30 -73.4 ± 10.5	-33.0 ± 1.82	1.8 ± 0.86
Holo-[12H:12L]	3.3 ± 0.13 3.3 ± 0.34	-49.8 ± 2.63	-53.5 ± 5.26	-33.8 ± 2.65	1.4 ± 0.24
Holo-[1H:23L]	0.8 ± 0.4	-47.0 ± 2.03	-55.5 ± 5.20 -	-55.0 ± 2.05	- 0.24
Holo-[19H:5L] (LB) (~200 Fe ^{III} /shell)	4.4 ± 0.64	-56.6 ± 3.95	-76.8 ± 7.71	-33.7 ± 3.96	1.4 ± 0.53
Holo-FtL [0H:24L]	_	_	_	_	_
Average		-54.5 ± 3.26	-70.3 ± 11.4	-33.6 ± 0.37	1.5 ± 0.22
Apo-NCOA4-D + Holo-Ferritin (LB) (~200 Fe ^{III} /shell)	n	ΔH (kJ/mol)	ΔS (J/mol·K) ^a	ΔG (kJ/mol) ^b	$K_a \times 10^{-6} (M^{-1})$
Holo-FtH [24H:0L]	6.2 ± 0.14	-20.8 ± 0.48	38.2 ± 2.32	-32.2 ± 0.44	1.3 ± 1.2
Holo-[19H:5L]	4.9 ± 0.43	-19.6 ± 0.56	40.2 ± 3.44	-31.6 ± 0.52	2.1 ± 1.1
Holo-[17H:7L]	4.1 ± 0.22	-26.5 ± 0.72	20.0 ± 2.85	-32.5 ± 0.77	1.6 ± 0.25
Holo-[16H:8L]	4.4 ± 0.55	-25.5 ± 0.78	28.5 ± 0.87	-34.0 ± 0.75	1.1 ± 0.38
Holo-[14H:10L]	3.0 ± 0.21	-26.2 ± 0.39	30.4 ± 1.58	-35.2 ± 0.38	0.8 ± 0.4
Holo-FtL [0H:24L]	_	_	_	_	_
Holo-FtH [24H:0L] (LB + 250 mg FeSO ₄ /L)	6.3 ± 0.33	-22.2 ± 1.38	33.5 ± 3.94	-32.2 ± 1.34	2.4 ± 0.97
Average		-23.5 ± 2.98	31.8 ± 7.30	-32.9 ± 1.36	1.6 ± 0.65

^a The entropy change ΔS is calculated from $\Delta G = \Delta H - T\Delta S$.

Fe—S cluster, although the specific cysteine residues involved in iron coordination are still unidentified [20]. This cluster was suggested to act as a cofactor for sensing intracellular iron levels, influencing the fate of NCOA4. In iron-depleted conditions, the absence of a Fe—S cluster disrupts this interaction, promoting ferritinophagy and iron release. Cellular oxygen levels were also found to affect NCOA4 and Fe—S cluster formation, with low oxygen promoting NCOA4 degradation and high oxygen triggering noncanonical autophagy of ferritin [21].

The role of NCOA4 in iron homeostasis is evident from knockout mice studies which show impaired iron release and erythropoiesis due to a lack of ferritin-stored iron in macrophages or hepatocytes [18,22]. Additionally, NCOA4 deficiency has been shown to increase the susceptibility to ferroptosis, a form of programmed cell death linked to lipid oxidation and relevant to neurodegenerative diseases and cancer [23,24]. Therapeutic strategies targeting ferritinophagy, such as inhibitors of the NCOA4-ferritin interaction could potentially treat conditions such as cardiomyopathies, stroke, and certain tumors [25,26].

In humans, the NCOA4 α variant, which includes the entire C-terminal subdomain (amino acid residues 383–522), is responsible for binding to ferritin and for ferritinophagy [18,27–29]. While ferritinophagy is thought to involve the full spectrum of iron-containing isoferritins (from heteropolymer H-rich to L-rich ferritins), it is unclear how the lysosomal degradation of homopolymer L-ferritin (FtL) or heteropolymer L-rich ferritin occurs, given the high specificity of NCOA4 recognition by ferritin H subunits, and by what process the L-rich ferritins release their load of iron and/or are brought to the lysosome for degradation. Additionally, it is currently unknown whether the Fe—S cluster is necessary for the NCOA4-ferritin interactions and what impact the iron content of ferritin and/or the size of the iron core have on this interaction.

To investigate these questions, we synthesized various recombinant ferritins, including homopolymer H-ferritin (FtH), homopolymer Lferritin (FtL), and heteropolymer ferritins with different H to L subunit ratios, in both their iron-free (apo) and iron-loaded (holo) forms. We also produced the soluble human NCOA4α variant in both its Fe-S cluster-bound form (holo-NCOA4-D, which shows a brown color upon purification) and its Fe—S -free form (apo-NCOA4-D, which is colorless), and used isothermal titration calorimetry (ITC) to examine the interactions between these different proteins. Our ITC results demonstrate significant differences in the binding thermodynamics, particularly the enthalpy change (ΔH) and entropy change (ΔS) of the reaction, while the binding stoichiometry and affinity remained essentially unchanged when apo- or holo-NCOA4-D was titrated against holo-ferritins. This indicates that the absence of the Fe-S cluster does not prevent the binding between NCOA4-D and ferritin but strongly influences the nature of the interaction. Specifically, we observed a significant change in the ΔH and ΔS values for the interactions between NCOA4-D and holoferritins from an average $\Delta H = -23.5 \pm 2.98$ kJ/mol and $\Delta S = 31.8 \pm$ 7.30 J K⁻¹ mol⁻¹ for apo-NCOA4-D to an average $\Delta H = -54.5 \pm 3.3$ kJ/ mol and $\Delta S = -70.3 \pm 11.4 \text{ J K}^{-1} \text{ mol}^{-1}$ for holo-NCOA4-D. In the presence of the Fe-S cluster, binding is driven by a more favorable enthalpy change and a significant decrease in entropy change, suggesting the formation of a more ordered complex and a key role for the Fe-S cluster in the structural organization of the complex. This enthalpy-entropy compensation process does not significantly affect the binding free energy ΔG (average of -33.25 ± 0.49 kJ/mol for both apoand holo-NCOA4-D binding to apo- and holo-ferritins), leading to similar apparent binding affinity Ka with an average value of (1.14 \pm $0.47) \times 10^5 \text{ M}^{-1}$ obtained from experimental ITC-fitted isotherms (Table 1). Furthermore, major differences were observed when holo-

 $[^]b$ The Gibbs free energy of binding (ΔG) is calculated using the equation $\Delta G=-RT$ ln Ka.

NCOA4-D was titrated against apo- and holo-ferritins with a reduced binding stoichiometry and lower ΔH and ΔS values for apo-ferritins, suggesting an important of the iron core in influencing the interactions between the two proteins (Table 1). Altogether, both the Fe—S cluster and the iron content of ferritin significantly affect the thermodynamics of the interactions between NCOA4-D and ferritins, contributing to an enhanced binding enthalpy and a more ordered and structured complex.

2. Materials and methods

2.1. Chemicals and reagents

All chemicals employed in this study were reagent grade and used purification. Tris-(hydroxymethyl)aminomethanehydrochloride (Tris-HCl), dibasic anhydrous sodium phosphate (Na₂HPO₄), ferrous sulfate heptahydrate (FeSO₄·7H₂O) were purchased from Fisher Scientific, and MOPS [3-(N-morpholino)propanesulfonic acid] was purchased from Research Organics (Cleveland, OH). Sodium chloride, ammonium sulfate, imidazole, sodium dithionite (also known as sodium hydrosulfite), and ferrozine were purchased from ACROS Organics, isopropyl \(\beta \)-1-thiogalactopyranoside (IPTG), and anhydrotetracycline (Tet) were purchased from Sigma-Aldrich (St. Louis, MO). Ferrous ions stock solutions were freshly prepared immediately before each experiment in a dilute HCl solution at pH 2.0. LB media broth was purchased from Alpha Teknova, Inc., and M9 media stock solutions were prepared in house and consisted of Na₂HPO₄.7H₂O (11.3 g), KH₂PO₄ (3.0 g), NaCl (0.5 g), NH₄Cl (1.0 g) dissolved in 1 L of DI water, adjusted to pH 7.4 and autoclaved. To this 1 L solution, filtered

solutions of 1 M MgSO $_4$ (2 ml), 1 M CaCl $_2$ (0.1 ml) and 10 ml of 20 % glucose were added. All solutions were filtered through 0.2 μ m Whatman Puradisc polyethersulfone sterile syringe filters (Cytiva) before use.

2.2. Recombinant ferritin expression and purification

The expression and purification of homopolymer and heteropolymer ferritin samples were performed using procedures that were established and optimized in our laboratory [14,30–33]. Briefly, recombinant human H ferritins (FtH) were produced in *E. coli* using pET vectors with a T7 promoter and pASK vectors with a Tet promoter, both conferring ampicillin resistance. Induction occurred in LB medium with 0.4 mM IPTG for 4 h at 37 °C. Recombinant human L ferritins (FtL) were expressed using pDS 20 vectors in the BL21 pLyS strain with M9 minimal medium for 7 h at 37 °C. Heteropolymer ferritins with different H to L subunit ratios were generated in *E. coli* Rosetta-gami B strain using a pWUR-FtH-TetO-FtL plasmid with varying inducer concentrations. Induction at 37 °C lasted 4–6 h using 10–1000 µM IPTG and 25–1600 ng/ml anhydrotetracycline, depending on the desired subunit ratio [30,31].

Cells were centrifuged, resuspended in Tris-HCl, sonicated, and centrifuged again. The supernatant was heat-treated at 80 °C, centrifuged, and then analyzed on SDS-PAGE. Proteins were precipitated with ammonium sulfate, dialyzed overnight, centrifuged, and purified using size exclusion chromatography. Purified ferritins were quantified using a Micro BCA Protein Assay Kit. A small iron core of $<\!200\pm50$ Fe(III)/ ferritin molecule was found in recombinant homopolymer H ferritin (FtH) and heteropolymer H/L ferritins produced in LB medium or homopolymer H and heteropolymer H/L ferritins produced in LB medium or homopolymer H and heteropolymer H/L ferritins produced in M9

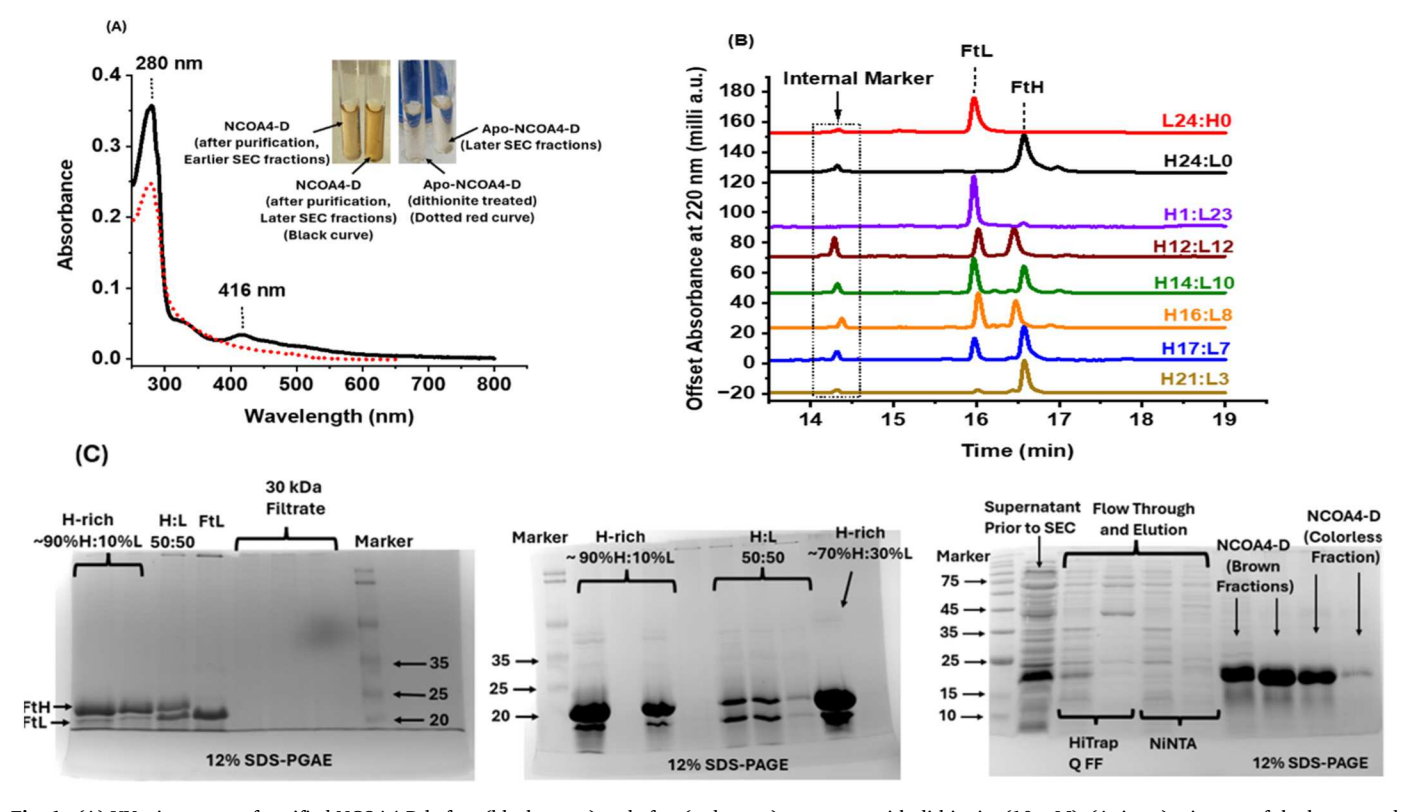


Fig. 1. (A) UV-vis spectra of purified NCOA4-D before (black curve) and after (red curve) treatment with dithionite (10 mM). (A, inset): pictures of the brown and colorless NCOA4-D fractions at various stages of the size exclusion chromatography (SEC) purification. (B) Capillary gel electropherograms (SDS-CGE) of recombinant human homopolymer H- and L-ferritin (100%H, 100%L, respectively), and of heteropolymer ferritins (~88%H:12%L or ~21H:3L, ~70%H:30%L or 17H:7L, ~67%H:33%L or 16H:8L, ~58%H:42%L or 14H:10L, ~50%H:50%L or 12H:12L, and ~5%H:95%L or 1H:23L), at protein concentrations between 0.5 and 0.8 mg/ml. The internal marker is a 10 kDa protein standard, provided with the SDS-MW Analysis Kit from Sciex.com, part number: 390953. (C) 12 % SDS-PAGE of purified ferritin and NCOA4 samples. The first two panels display the electrophoretic mobilities of different heteropolymer ferritin samples having different compositions of H and L subunits used in this study. The right panel displays the mobility of our NCOA4 samples, both with and without the Fe—S cluster (brown and colorless fractions, respectively), after size exclusion chromatography and anion exchange coupled with affinity chromatography (see Materials and methods for more details).

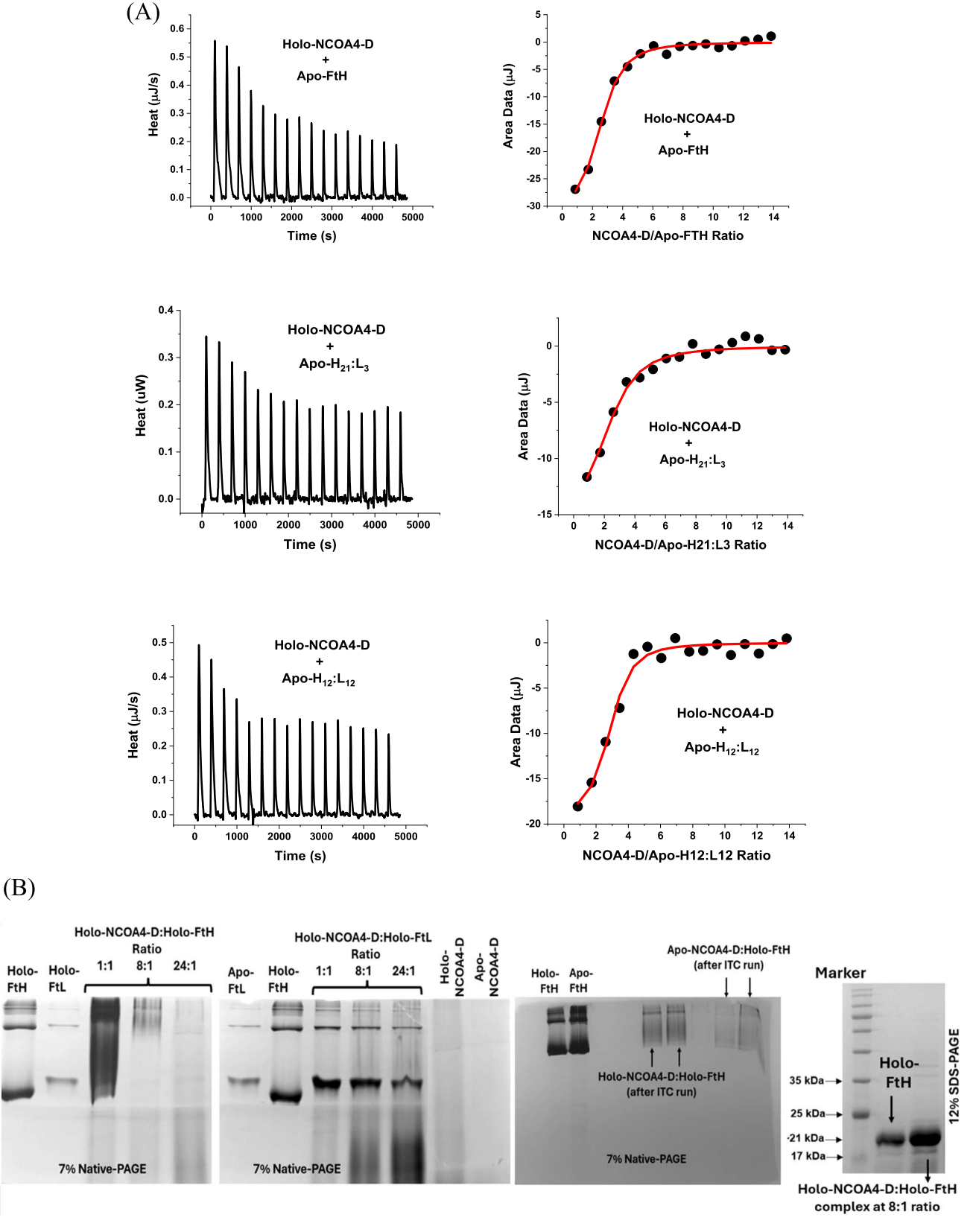


Fig. 2. (A) Calorimetric titrations of holo-NCOA4-D (containing a Fe—S cluster) with homopolymer H-ferritin, FtH, and heteropolymer ferritins at the indicated H to L subunit ratios, and plots of the integrated heats (Area Data) vs. the NCOA4:ferritin molar ratio. Conditions: $3.0 \mu M$ (FtH and 21H:3L) and $5.0 \mu M$ (12H:12L) ferritin samples titrated with 3 μ l injections of $150 \mu M$ NCOA4-D, in 100 mM sodium phosphate and 100 mM NaCl, pH 7.4 and $25.00 \,^{\circ}$ C. All purified ferritin samples were produced in M9 medium and contained <50 iron atoms per ferritin molecule (i.e., apo-ferritins). (B) 7 % native- and 12%SDS-PAGE of NCOA4-D-ferritin interactions studied by EMSA with conditions indicated above each lane.

minimal medium contained $<50\pm10$ Fe(III)/ferritin molecule, as determined by an iron reductive mobilization assay [34,35].

2.3. Expression and purification of human NCOA4 domain (383–522)

The pET-12a/hNCOA4 (383–522) plasmid was used to transform BL21 (DE3) pLys strain of *E. coli* and expression was induced in an LB medium using 0.4 mM isopropyl β -D-1-thiogalactopyranoside (IPTG) at 37 $^{\circ}$ C for 4 h. The bacteria pellet was re-suspended in 20 mM Na₂HPO₄, 100 mM NaCl pH 6.2 and sonicated for 2 cycles at 5 min each and 50–60 % amplitude. The protein sample was then loaded on a HiTrap Q HP or a HiTrap Q FF strong anion exchange chromatography columns (Cytiva)

equilibrated with 20 mM Na_2HPO_4 , 100 mM NaCl pH 6.2. The flow through fractions containing the NCOA4 domain protein (NCOA4-D, aa 383–522) were re-loaded on a Ni-NTA column equilibrated with 20 mM Na_2HPO_4 , 100 mM NaCl, pH 6.2 and eluted with a linear imidazole gradient 0–0.5 M in 20 mM Na_2HPO_4 , 500 mM NaCl, pH 6.2 buffer. The fractions that contained recombinant human NCOA4-D (brown color) were collected and concentrated using a 10 kDa cut-off Amicon concentrator, maintained at 4–8 °C. To obtain a colorless NCOA4-D without the iron-sulfur cluster, the solution was treated for 30 min with 10 mM dithionite under a positive atmosphere of argon, washed several times with buffer, and then thoroughly dialyzed overnight into the final working buffer.

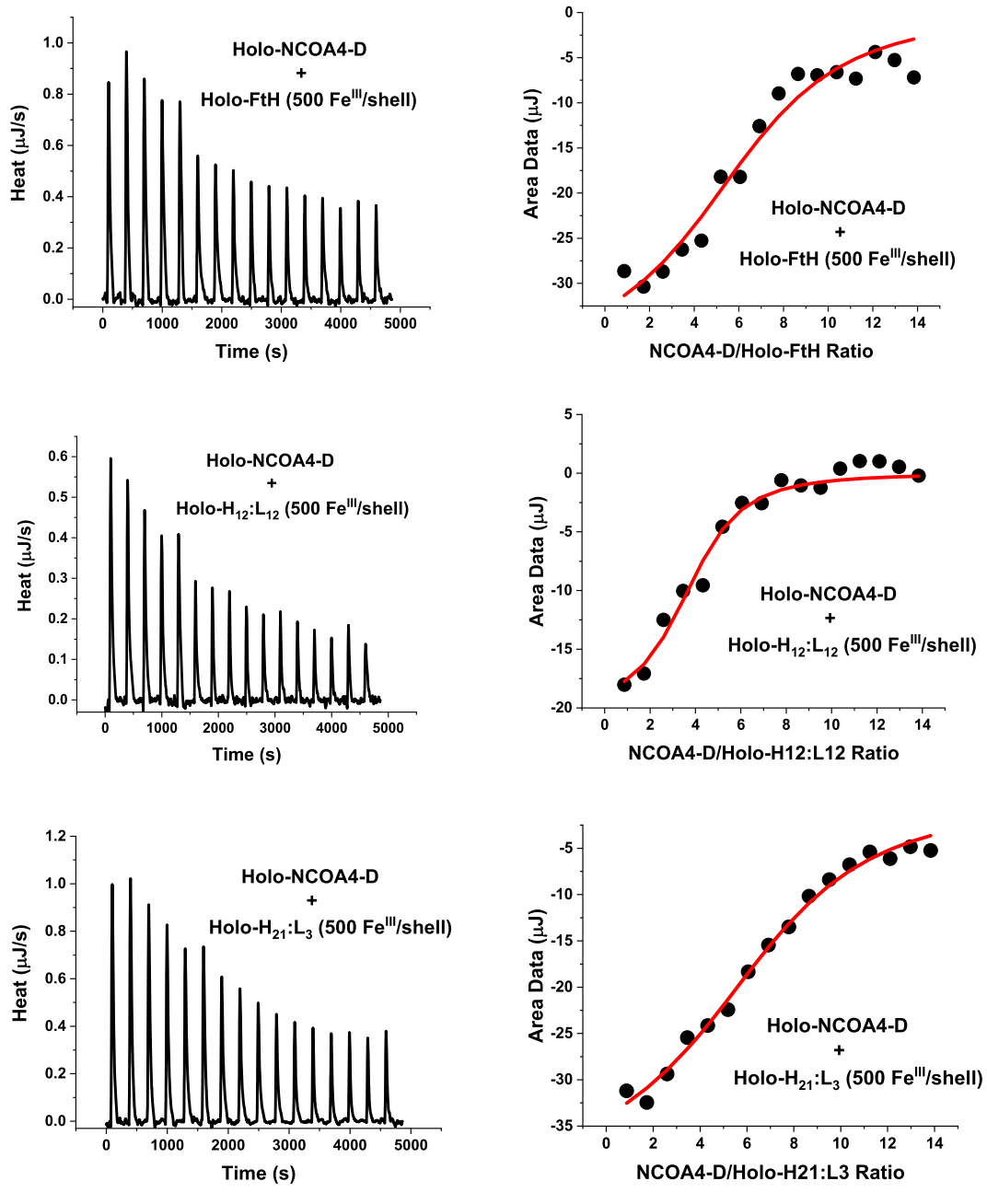


Fig. 3. Calorimetric titrations of holo-NCOA4-D (containing a Fe—S cluster) with homopolymer H- and L-ferritins (FtH and FtL, respectively) and heteropolymer ferritins at the indicated H to L subunit ratios, and plots of the integrated heats vs. the NCOA4:ferritin molar ratio. Conditions: $3.0 \,\mu\text{M}$ ferritin samples titrated with 3 μ l injections of 150 μ M NCOA4-D, in 100 mM sodium phosphate and 100 mM NaCl, pH 7.4 and 25.00 °C. All purified ferritin samples were produced in LB medium and were further loaded with exogenous iron (one injection of 300 Fe^{II}/shell) and have an average iron core of \sim 500 Fe^{III}/shell. The exception is the H-rich ferritin sample 80%H:20%L or 19H:5L which was not treated with exogenous iron and thus contained an average iron core of \sim 200 Fe^{III}/shell. These ferritin samples are referred to as holo-ferritins.

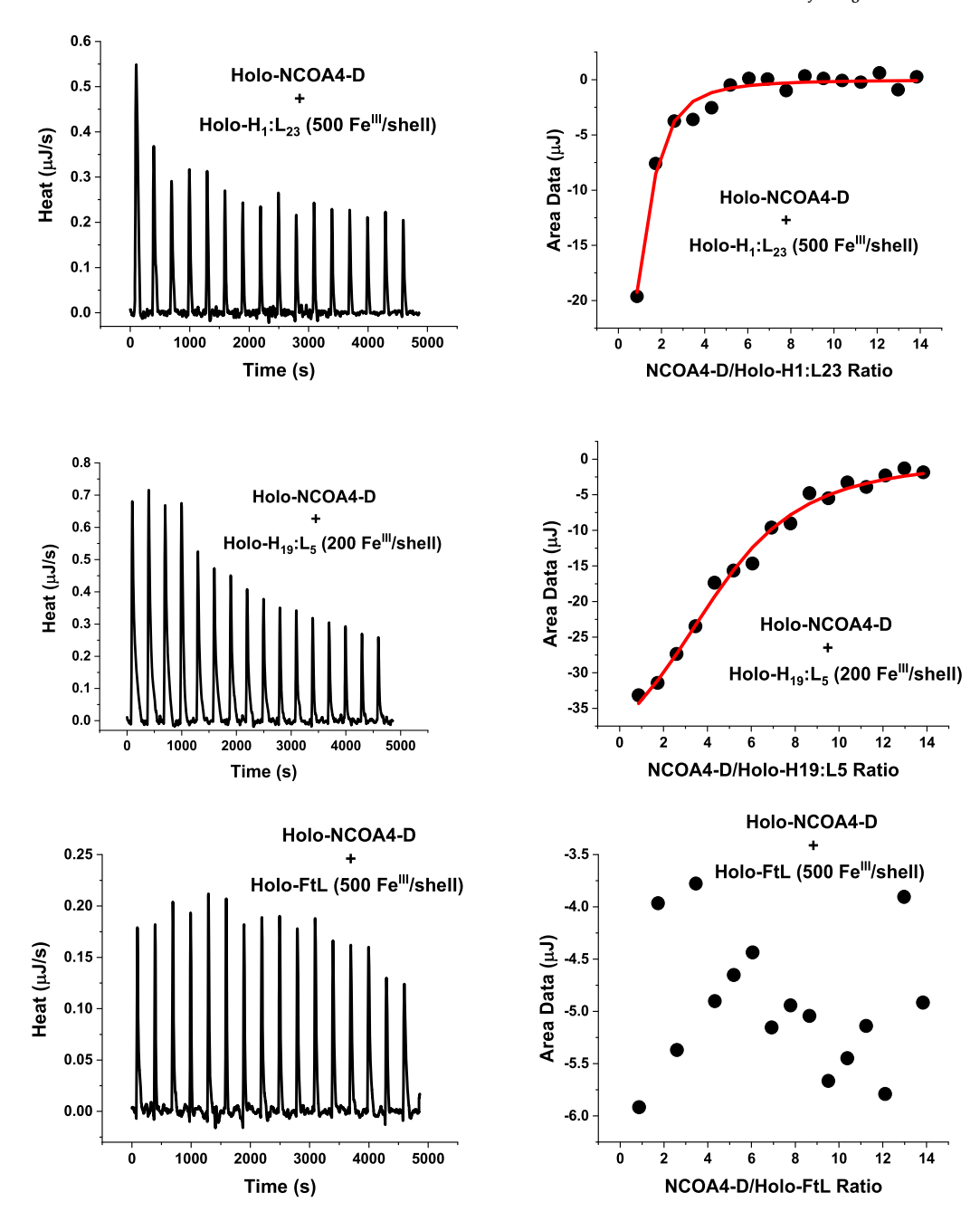


Fig. 3. (continued).

2.4. Native and SDS gel electrophoresis, and SDS-capillary gel electrophoresis (SDS-CGE)

Native-PAGE (7 % acrylamide) stained with Coomassie blue (Sigma-Aldrich) and gel electrophoresis mobility shift assays (EMSA) were used to investigate the interactions between ferritin and NCOA4-D using different ratios of NCOA4-D and ferritin. SDS-PAGE gels (12 % acrylamide) with densitometry analysis (Bio-Rad system) were used to examine the integrity of the ferritin samples and to estimate the ferritin subunit composition from band intensities. To more accurately quantify the H and L subunit composition of purified recombinant human homopolymer and heteropolymer ferritins, capillary gel electrophoresis experiments were performed under denaturing conditions (SDS-CGE) using an Agilent Technologies 7100 model capillary electrophoresis (CE) instrument. The procedure and the detailed conditions have been published in previous papers from our lab [14,29–31]. Briefly, a Sciex

SDS-CGE analysis kit and an Agilent Technologies 50 μ m ID bare fused silica capillary were used in these experiments. The capillary was preconditioned with a series of high-pressure washes and conditioning using NaOH, HCl, water, and SDS gel buffer. Protein samples (typically 100 μ l at 1–2 mg/ml) were prepared in SDS sample buffer (>60 % by volume) with 2-beta-mercaptoethanol (5 % (ν / ν)), heated at 100 °C, cooled to room temperature, and then injected electro-kinetically on the CE instrument. Ferritin H and L subunit separation occurred under a negative applied voltage with pressure maintained at 2.0 bar and a temperature of 25 °C. Detection was set at a wavelength of 220 nm, with a reference wavelength of 350 nm and a response time of 1.0 s.

2.5. Isothermal titration calorimetry (ITC)

ITC experiments were performed using a TA Instruments small-volume Nano ITC instrument with gold cells and an active cell volume

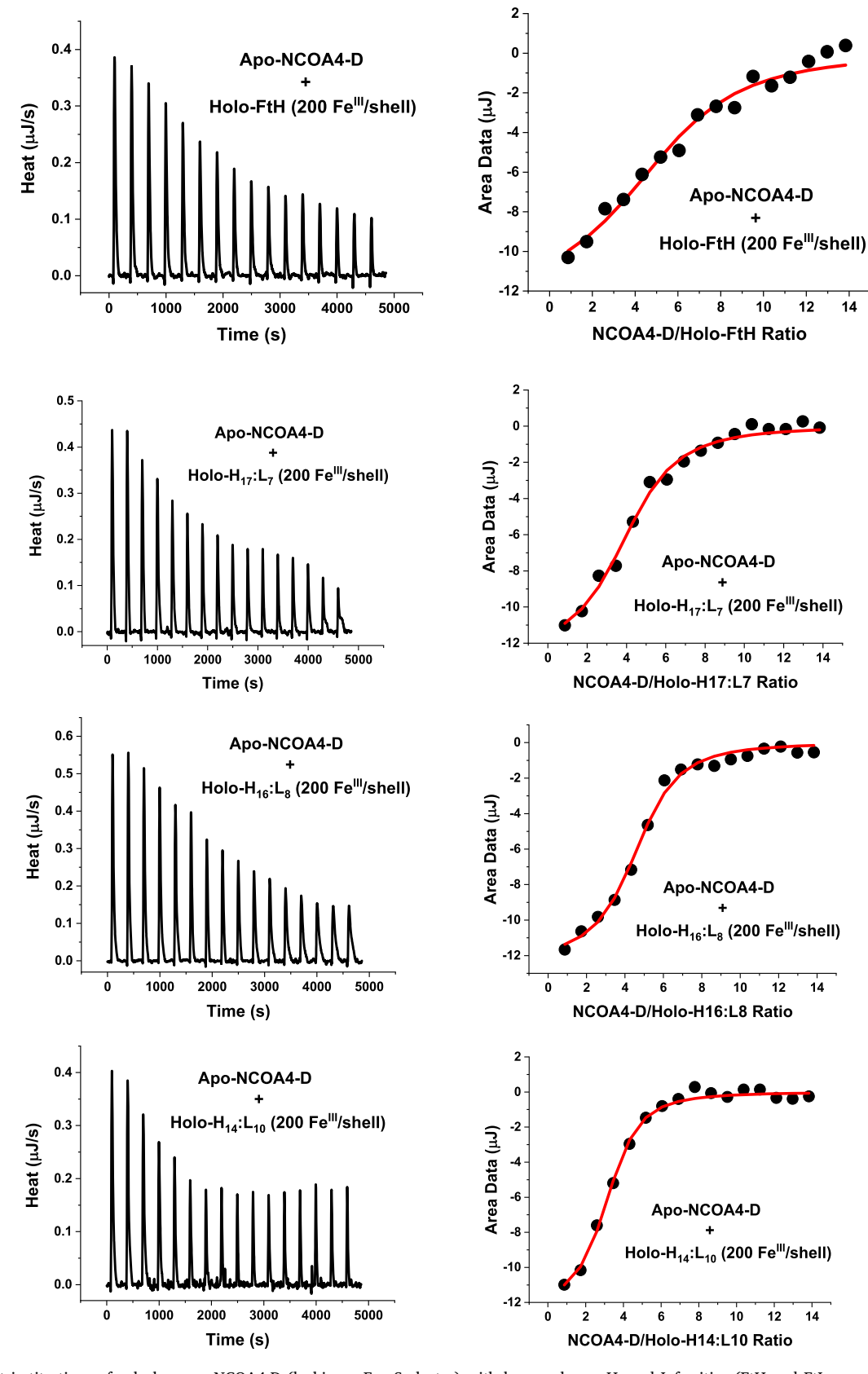


Fig. 4. Calorimetric titrations of colorless apo-NCOA4-D (lacking a Fe—S cluster) with homopolymer H- and L-ferritins (FtH and FtL, respectively) and heteropolymer ferritins at the indicated H to L subunit ratios, and plots of the integrated heats vs. the NCOA4:ferritin molar ratio. Conditions: $3.0 \mu M$ ferritin samples titrated with 3μ l injections of $160 \mu M$ NCOA4-D, in $100 \mu M$ sodium phosphate and $100 \mu M$ NaCl, pH 7.4 and 25.00 °C. All purified ferritin samples were produced in LB medium and contained about $200 \mu M$ Fe^{III}/shell iron core, with the exception of a holo-ferritin sample (holo-FtH) produced in LB medium supplemented with $250 \mu M$ medium sulfate per liter of culture.

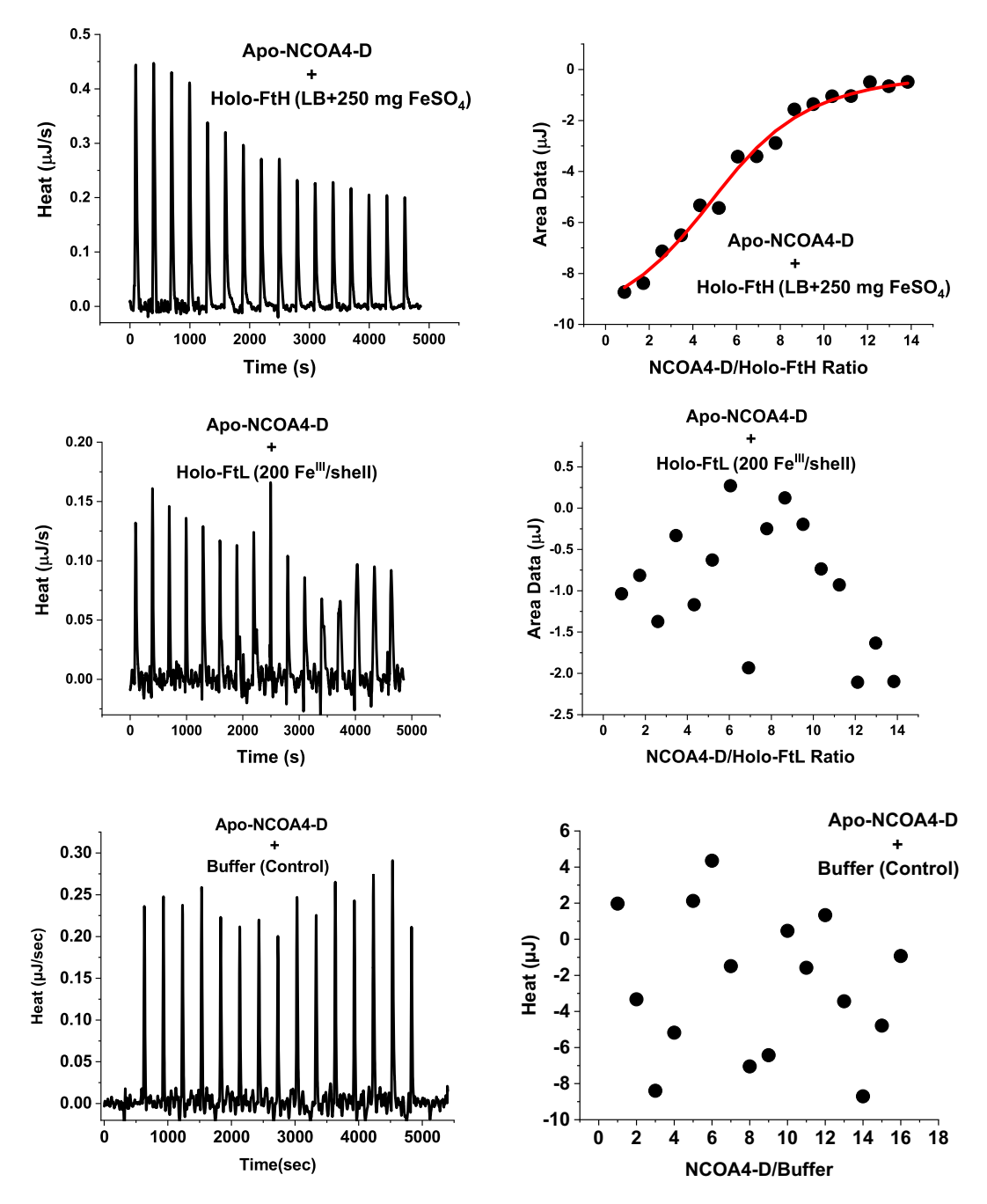


Fig. 4. (continued).

of 185 µl. The association constant (Ka), stoichiometry (n), and enthalpy change (ΔH) of the reaction were simultaneously and directly measured in a single ITC experiment. The Gibbs free energy of binding (ΔG) was calculated using $\Delta G=-RT$ ln Ka, and the enthalpy change (ΔS) was calculated from the equation $\Delta G=\Delta H-T\Delta S$. All titrations were conducted at 25.00 °C in a buffer of 100 mM sodium phosphate, 100 mM NaCl, pH 7.4, with a stirring rate of 250 rpm and a 50 µl titrating syringe. Each ITC experiment consisted of an automated sequence of 16 injections, 3 µl each, of an NCOA4-D working solution into the sample cell containing ferritin. Injections were spaced 5 min apart to allow for complete equilibration, with the equivalence point occurring at the midpoint of the titration area. Data were collected and analyzed using Nano-Analyze software from TA Instruments, employing a model of one class of independent binding sites. Experiments were repeated two to three times on average to ensure reproducibility, with a background

correction in the absence of ferritin to account for the heat of mixing and dilution. Standard errors from replicate determinations are indicated in Table 1, and specific conditions for each experiment are detailed in the figure captions.

3. Results

3.1. Characterization of purified NCOA4-D and ferritin samples

The UV-vis spectrum of purified NCOA4-domain (383–522), NCOA4-D, revealed an intense brown color with a main peak at \sim 416 nm and broad shoulders at \sim 455 nm and \sim 500 nm (Fig. 1A) characteristic of iron-sulfur clusters [36,37]. These peaks along with the protein's brown color disappeared after treatment with dithionite, suggesting reduction and loss of the Fe—S clusters (Fig. 1, inset) and that

the iron-sulfur cluster is redox-active. As expected, a band for purified NCOA4-D appears at $\sim\!17$ kDa on 12 % SDS-PAGE (Fig. 1C). Similarly, heteropolymer ferritin samples showed two bands on 12 % SDS-PAGE, corresponding to the H and L subunits with the gel band intensities corresponding to the expected H:L subunit ratio.

To confirm and accurately quantify the ferritin H to L subunit ratio, SDS-CGE experiments were conducted and showed well-resolved peaks of the L and H subunits. From the area under the CGE peaks, the subunit composition of heteropolymer ferritins was calculated with the H and L subunit ratio displayed next to each electropherogram in Fig. 1B.

3.2. Isothermal titration calorimetry (ITC) of NCOA4-D and ferritin interactions

To investigate the interactions between NCOA4-D and ferritin, ITC experiments were performed using both colored and colorless NCOA4-D and different types of ferritin (apo-ferritin without an iron core, holoferritin with an iron core, homopolymer H- (FtH) and L-ferritin (FtL), and heteropolymer ferritins of different H to L subunit ratios). In this study, we refer to colored NCOA4-D samples as "Holo-NCOA4-D", and colorless NCOA4-D samples as "Apo-NCOA4-D" to illustrate the presence or absence of the Fe—S cluster in NCOA4-D, respectively. In all ITC experiments, recombinant human ferritin was placed in the ITC sample cell (185 µl cell volume) and titrated sequentially with 3 µl injections of NCOA4-D preloaded into the 50 µl injection syringe. The raw calorimetric data (μ J/s), and the integrated heats (μ J) for each injection versus the molar ratio of NCOA4-D to ferritin, after subtraction of the heat of dilution, are illustrated in Figs. 2–4. Notably, the reaction heats from the titration of NCOA4-D into homopolymer L-ferritin (FtL) are very similar to those obtained when NCOA4-D is titrated into buffer, suggesting no association between NCOA4-D and L-ferritin, as previously found [29].

3.3. Holo-NCOA4-D binding to homopolymer and heteropolymer ferritins

3.3.1. Holo-NCOA4-D binding to apo-ferritins

To investigate whether the binding of NCOA4-D requires the presence of an iron core inside ferritin, ITC experiments were initially performed with ferritin samples that lacked an iron core (apo-ferritin with <50 Fe^{III} atoms per ferritin molecule). These apo-ferritin samples were produced in an iron-free M9 minimal medium and did not exhibit the typical yellow color, which usually indicates the presence of a sizeable iron core. Additionally, a ferritin iron reductive mobilization assay using the non-enzymatic FMN/NADH system [11,35] and the strong ferrous ion chelator, ferrozine [34], showed <50 iron atoms per ferritin molecule (data not shown), suggesting essentially an iron core-free ferritin.

ITC titrations of holo-NCOA4-D with homopolymer H-ferritin without an iron core (apo-FtH) revealed ITC upward positive peaks, corresponding to an exothermic reaction (Fig. 2), with the heats at the end of the reaction being similar to those of the control experiment (i.e., dilution of NCOA4-D into buffer). Accordingly, the data was curve-fitted using a model of one set of independent binding sites. Excellent fits were achieved with an average binding stoichiometry (n) of 2.4 \pm 0.2 NCOA4-D molecule per ferritin shell and an average apparent binding affinity of \sim (1.3 \pm 1.1) \times 10⁶ M⁻¹ (Table 1). The average enthalpy and entropy changes of the reaction were $\Delta H \sim -49.9 \pm 0.88$ kJ/mol and $\Delta S \sim -58.6 \pm 0.68 \ J \ K^{-1} \ mol^{-1}.$ The large and negative ΔH and ΔS values suggest an exothermic/energetically favorable reaction and the formation of an ordered system, and are typically due to structural stabilization, desolvation effects, and the formation of a more rigid and structured complex. A similar pattern is observed with heteropolymer ferritin samples in their apo-forms (i.e. 88%H:12%L or ~21H:3L, and 50%H:50%L or 12H:12L), as shown in Table 1. Since NCOA4-D binds exclusively to ferritin H subunits, the 12H:12L sample exhibited a lower binding stoichiometry, as expected, due to the reduced number of available H subunits (Table 1).

To investigate the interactions between the two forms of NCOA4-D

(with and without the Fe—S cluster), we performed gel electrophoresis mobility shift assays (EMSA) using various NCOA4-D to ferritin ratios (Fig. 2B). The EMSA results revealed upward-shifted bands for the 1:1, 1:8, and 24:1 NCOA4-D to ferritin ratios, with no visible bands for ferritin alone, indicating the formation of a higher molecular weight complex between NCOA4-D and ferritin, in support of the ITC results. As expected, no mobility shift was observed with homopolymer L ferritin (FtL), confirming the exclusive interactions between NCOA4-D and ferritin H subunits. Samples taken at the end of the ITC titrations also showed an EMSA mobility shifts similar to the "pre-prepared" complexes, confirming the formation of NCOA4-D-ferritin complexes. On denaturing SDS-PAGE, both NCOA4-D and ferritin showed similar mobility, resulting in a single intense band around 21 kDa (Fig. 2B), corresponding to the dissociated ferritin and NCOA4-D, consistent with the earlier results shown in Fig. 1C.

3.3.2. Holo-NCOA4-D binding to holo-ferritins

In another series of ITC experiments, holo-NCOA4-D was titrated into solutions of holo-ferritin (both H- and L-homopolymers, FtH and FtL, and H/L heteropolymers including 88%H:12%L or ~21H:3L, 50% H:50%L or 12H:12L, and 5%H:95%L or ~1H:23L) containing an iron core of ~500 Fe^{III}/shell. These holo-ferritins were produced in LB medium and initially contained \sim 200 Fe^{III}/shell. They were loaded in vitro with exogenous iron (one injection of 300 Fe^{II}/shell) to obtain the aforementioned holo-ferritin samples with an average iron core size of ${\sim}500~\text{Fe}^{\text{III}}\!/\text{shell}.$ The holo-H-homopolymer (holo-FtH) and the 21H:3L heteropolymer samples showed the highest binding stoichiometry of ~5-6 NCOA4-D molecules per ferritin shell, followed by the 12H:12L sample (~3 NCOA4-D per ferritin shell). As expected, no detectable binding isotherms were observed with holo-NCOA4-D titration against holo-L-ferritin; however, heats of binding were observed with a holo-Lrich ferritin (i.e. 1H:23L), suggesting that the presence of at least 1 H subunit in ferritin is sufficient for interactions with NCOA4-D (Fig. 3). However, the thermodynamic parameters in this latter case could not be determined accurately due to the few numbers of peaks defining the binding isotherm. A similar ITC isotherm and binding thermodynamics were obtained with a heteropolymer ferritin sample (i.e. 80%H:20%L or 19H:5L) produced in LB with an iron core of about 200 Fe^{III}/shell (Fig. 3, Table 1) but without exogenously added iron. Compared to the results with the apo-ferritin samples, the presence of an iron core enhanced the binding interactions with holo-NCOA4-D, displaying higher binding stoichiometries, and an increase in the ΔH and ΔS values (both negative). The higher values for both ΔH and ΔS (Table 1) highlight the distinct nature of the interactions between holo-NCOA4-D and holoferritins, compared to holo-NCOA4-D and apo-ferritins, and indicate stronger or additional binding interactions and a more ordered or structured binding.

3.3.3. Apo-NCOA4-D binding to holo-ferritins

To explore whether the presence of an Fe-S cluster on NCOA4-D influences the interaction with ferritins, ITC experiments were designed utilizing both homopolymer H- and L-ferritins, and heteropolymer ferritins including 70%H:30%L or 17H:7L, 67%H:33%L or 16H:8L, and 58%H:62%L or 14H:10L, each containing ${\sim}200~\text{Fe}^{\text{III}}/\text{shell}$ iron core. The results show a decrease in the ΔH values (from $\sim\!-55$ kJ/ mol in the case of holo-NCOA4-D to \sim 24 kJ/mol in the case of apo-NCOA4-D), suggesting that the Fe—S cluster enhances bond formation and strengthens the association of NCOA4-D with ferritin (Fig. 4, Table 1). Additionally, the ΔS values switched from large and negative (i.e. $\sim\!-70~\text{JK}^{-1}~\text{mol}^{-1}$ in the case of holo-NCOA4-D) to small and positive (i.e. $\sim +32 \text{ JK}^{-1} \text{ mol}^{-1}$ in the case of apo-NCOA4-D), reinforcing the notion of a weaker interaction between apo-NCOA4-D and holoferritins and thus a role for the Fe-S cluster in strengthening the association between holo-NCOA4- and ferritins (Fig. 4, Table 1). The differences in the ΔH and ΔS values between the apo- and the holo-forms of NCOA4-D highlight the distinct nature of the interactions involved.

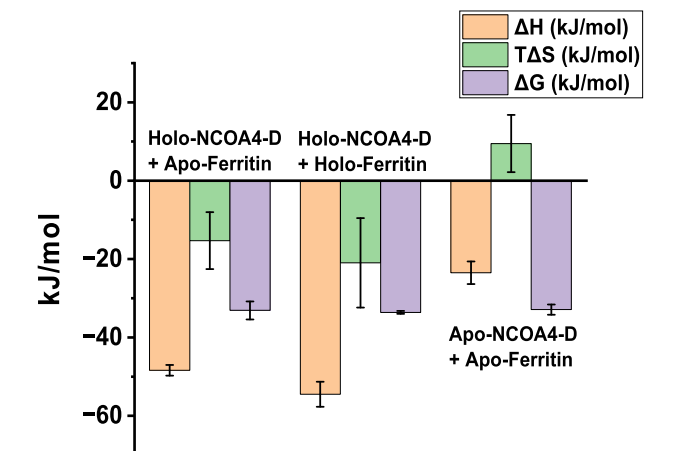


Fig. 5. Summary of the thermodynamic results from all ITC titrations reported in Figs. 2, 3, 4 and Table 1.

Without the Fe—S cluster, the binding is driven by favorable enthalpy change and increased disorder, while with the Fe—S cluster the binding is driven by even more favorable enthalpy at the cost of further decrease in entropy due to an increased order in the system. Similar results were obtained with a ferritin sample produced in an LB medium supplemented with 250 mg ferrous ammonium sulfate per liter of culture (Table 1). The purpose of supplementing the LB medium with exogenous iron is to determine if differences in binding thermodynamics can be observed between a ferritin sample loaded with exogenous iron, after purification, and a ferritin sample produced in LB medium supplemented with exogenous iron, simulating iron overload conditions. Overall, our results demonstrate that the presence of the Fe—S cluster significantly impacts the thermodynamics of the binding interactions between NCOA4-D and ferritin, making the association stronger and

more ordered.

4. Discussion

NCOA4-mediated ferritinophagy is an essential mechanism for normal iron homeostasis that involves the binding of NCOA4 to ferritin H subunits, leading to the release of the iron stored inside ferritin [27,38]. Dysregulation of NCOA4 is associated with several pathological conditions, including neurodegenerative diseases, ischemia/reperfusion injury, and cancer [19]. The lysosomal degradation of ferritin by the selective autophagy adaptor NCOA4 is essential for iron bioavailability and utilization in processes like heme and iron-sulfur cluster biosynthesis [16]. When iron levels are low, ferritin is transported to lysosomes either via NCOA4-driven macro-autophagy or a noncanonical pathway triggered by iron-induced condensation of NCOA4 during prolonged iron-replete conditions [27,38,39]. Hyperoxic conditions also trigger ferritinophagy through iron-induced NCOA4 condensation, while hypoxic conditions promote the incorporation of an Fe—S cluster into NCOA4, leading to its degradation by HERC2 [21].

Earlier studies have explored the interactions between NCOA4-D and ferritin, demonstrating a strong affinity between the two proteins [28,29]. However, these studies have not examined the role (if any) of the Fe—S cluster bound to NCOA4-D, or the effects of ferritin H and L subunit composition and ferritin iron content on the binding interactions between the two proteins. A more recent cryo-EM structure from our laboratory identified several key amino acids on NCOA4-D and FtH that are essential for their interaction [40]. The cryo-EM structure elucidated the reason for the binding selectivity of NCOA4-D towards ferritin's H subunits and revealed the structural basis of NCOA4-mediated ferritinophagy [40]. Other studies [20,21] revealed that the presence of an Fe—S cluster on NCOA4 acts as a cofactor for sensing intracellular iron levels and dictates the fates of NCOA4 and ferritin. While structural data for the Fe-S-NCOA4 complex is currently lacking, site-directed mutagenesis showed that four cysteine residues (C404,

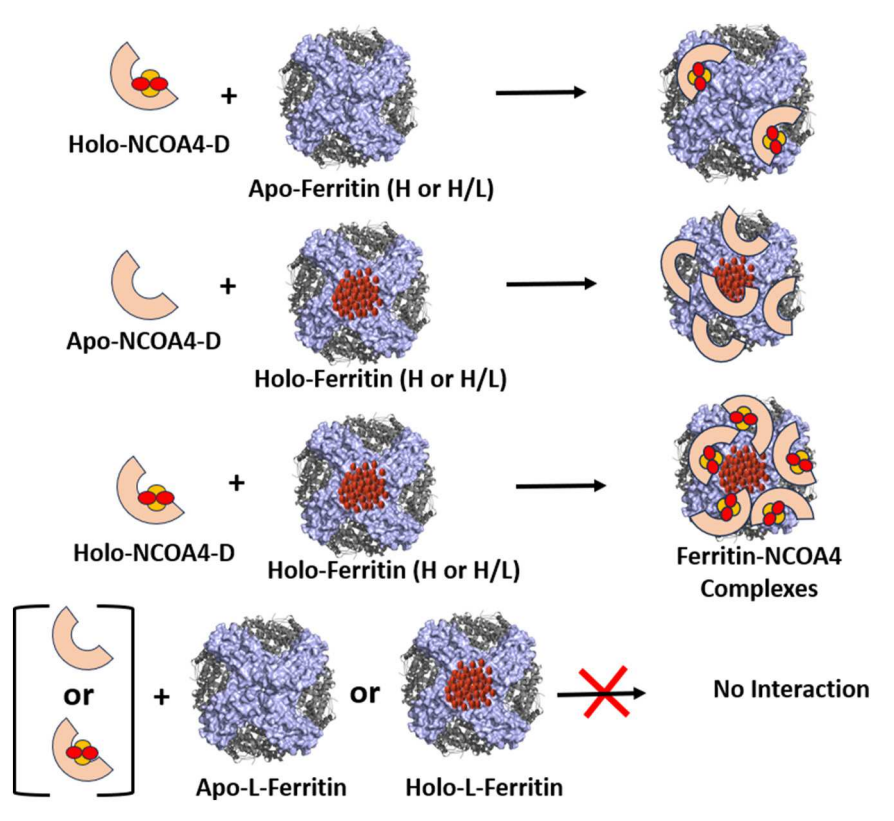


Fig. 6. Schematic illustration of NCOA4-D interaction with ferritin in-vitro.

C410, C416, and C422) are crucial for the formation of the iron-sulfur cluster in NCOA4 [20,21]. The removal of the Fe-S cluster from NCOA4 is likely to induce a conformational change in the protein, as suggested by Kuno et al. [39], who found that the interaction between NCOA4 and HERC2 was governed by an iron-dependent conformational change in NCOA4. However, further research is needed to confirm this. Moreover, in a previous study from our laboratory [29], we showed that iron mobilization from ferritin by reducing agents was inhibited by NCOA4 concentration, suggesting that NCOA4 binding to ferritin may disrupt electron transfer reactions through the ferritin shell. However, further research is needed to explore in more details potential redox reactions involved between the Fe-S cluster in NCOA4 and the ferritin iron cores. In this work, we employed isothermal titration calorimetry (ITC) to explore the interactions between NCOA4-D and various ferritins (homopolymers and heteropolymers) and elucidate the effect of ferritin iron loading and ferritin H/L subunit composition, as well as the role of the Fe—S cluster on the thermodynamics of these interactions.

Our ITC experiments demonstrated significant differences in the binding thermodynamics between NCOA4-D (with and without the Fe—S cluster) and various forms of ferritins (i.e. homopolymers, heteropolymers, iron-free, and iron-loaded ferritins). Overall, the binding reactions between NCOA4-D and ferritins (both in their apo and holo forms) exhibited exothermic and energetically favored reactions (i.e. negative ΔH). However, a large and negative ΔS of reaction was observed with holo- but not apo-NCOA4-D, suggesting a more ordered and structured system and an important role for the Fe-S cluster in stabilizing the complex (Table 1, Fig. 5). Additionally, the presence of a ferritin iron core enhanced the binding thermodynamics between NCOA4-D and ferritin, as evidenced by the further increase in the values of both ΔH and ΔS (Table 1). To better visualize the interactions between NCOA4-D and ferritin, we created a schematic illustration of these reactions, as depicted in Fig. 6. In vitro studies have shown that ironloaded ferritins are 10 to 20 °C less stable than apo-ferritin [30]. It has been proposed that this reduced thermal stability may result from structural destabilization around the 3-fold channels with potentially significant physiological implications [30]. For instance, the level of ferritin iron loading could serve as a sensor or be involved in cellular signaling pathways that trigger ferritin degradation and iron recycling. It remains unknown whether similar structural modifications also occur in vivo and whether specific biomolecules or cellular regulators are required to recognize these changes. Such processes could either (1) expose the ferritin iron mineral to cellular reductants to maintain iron homeostasis, (2) direct the ferritin molecule for lysosomal degradation and iron release, or (3) sequester ferritin as lysosomal hemosiderin if iron is in excess and not needed for cellular use. One stimulating possibility is that NCOA4 might act as the cellular regulator capable of sensing or detecting small structural or conformational changes in ferritin and the increasing iron levels inside the ferritin cavity, thereby triggering its interaction with ferritin and ultimately ferritinophagy.

Overall, our findings highlight the critical role of the Fe—S cluster and ferritin iron content in modulating the binding interactions between NCOA4-D and ferritin. They provide important insights into the molecular mechanisms underlying NCOA4-ferritin interactions and the potential regulatory function that Fe—S cluster, and the ferritin iron core, may exert during the process of ferritinophagy.

CRediT authorship contribution statement

Fadi Bou-Abdallah: Writing – review & editing, Writing – original draft, Validation, Supervision, Software, Resources, Project administration, Methodology, Investigation, Funding acquisition, Formal analysis, Data curation, Conceptualization. Mohamed Boumaiza: Writing – review & editing, Validation, Methodology, Investigation, Data curation. Ayush K. Srivastava: Writing – review & editing, Validation, Supervision, Methodology, Investigation.

Declaration of competing interest

The authors declare that they have no known competing financial interests or personal relationships that could have appeared to influence the work reported in this paper.

Data availability

The data that has been used is confidential.

Acknowledgement

This research is supported by NSF-BSF award # 2231900 from the Division of Molecular and Cellular Biosciences.

References

- S.J. Dixon, B.R. Stockwell, The role of iron and reactive oxygen species in cell death. Nat. Chem. Biol. 10 (2014) 9–17.
- [2] S. Altamura, O. Marques, S. Colucci, C. Mertens, K. Alikhanyan, M. U. Muckenthaler, Regulation of iron homeostasis: lessons from mouse models, Mol. Asp. Med. 75 (2020) 100872.
- [3] A.R. Bogdan, M. Miyazawa, K. Hashimoto, Y. Tsuji, Regulators of iron homeostasis: new players in metabolism, cell death, and disease, Trends Biochem. Sci. 41 (2016) 274–286.
- [4] T. Ganz, E. Nemeth, Hepcidin and iron homeostasis, Biochim. Biophys. Acta 1823 (2012) 1434–1443.
- [5] D.L. Zhang, M.C. Ghosh, T.A. Rouault, The physiological functions of iron regulatory proteins in iron homeostasis - an update, Front. Pharmacol. 5 (2014) 124
- [6] C. Renassia, C. Peyssonnaux, New insights into the links between hypoxia and iron homeostasis, Curr. Opin. Hematol. 26 (2019) 125–130.
- [7] D. Watts, D. Gaete, D. Rodriguez, D. Hoogewijs, M. Rauner, S. Sormendi, B. Wielockx, Hypoxia pathway proteins are master regulators of erythropoiesis, Int. J. Mol. Sci. 21 (2020).
- [8] F. Bou-Abdallah, The iron redox and hydrolysis chemistry of the ferritins, Biochim. Biophys. Acta, Gen. Subj. 1800 (8) (2010) 719–731.
- [9] P.M. Harrison, P. Arosio, Ferritins: molecular properties, iron storage function and cellular regulation, Biochim. Biophys. Acta 1275 (1996) 161–203.
- [10] A. Melman, F. Bou-Abdallah, Iron mineralization and core dissociation in mammalian homopolymeric H-ferritin: current understanding and future perspectives, Biochim. Biophys. Acta 1864 (11) (2020) 129700.
- [11] F. Bou-Abdallah, J.J. Paliakkara, G. Melman, A. Melman, Reductive mobilization of iron from intact ferritin: mechanisms and physiological implication, Pharmaceuticals 11 (4) (2018) 120.
- [12] P. Arosio, L. Elia, M. Poli, Ferritin, cellular iron storage and regulation, IUBMB Life 69 (2017) 414–422.
- [13] F.M. Torti, S.V. Torti, Regulation of ferritin genes and protein, Blood 99 (2002) 3505–3516.
- [14] A.K. Srivastava, A.A. Reutovich, N.J. Hunter, P. Arosio, F. Bou-Abdallah, Ferritin microheterogeneity, subunit composition, functional, and physiological implications, Sci. Rep. 13 (2023) 19862.
- [15] B. Chiou, R.J. Connor, Emerging and dynamic biomedical uses of ferritin, Pharmaceuticals 11 (4) (2018) 124.
- [16] B. Galy, M. Conrad, M. Muckenthaler, Mechanisms controlling cellular and systemic iron homeostasis, Nat. Rev. Mol. Cell Biol. 25 (2024) 133–155.
- [17] R. Bellelli, G. Federico, A. Matte, D. Colecchia, A. Iolascon, M. Chiariello, M. Santoro, L. De Francheschi, F. Carlomango, NCOA4 deficiency impairs systemic iron homeostasis, Cell Rep. 14 (2016) 411–421.
- [18] J.D. Mancias, L.P. Vaites, S. Nissim, D.E. Biancur, A.J. Kim, X. Wang, Y. Liu, W. Goessling, A.C. Kimmelman, J.W. Harper, Ferritinophagy via NCOA4 is required for erythropoiesis and is regulated by iron dependent HERC2-mediated proteolysis, Elife 4 (2015) 1–19.
- [19] N. Santana-Codina, J.D. Mancias, The role of NCOA4-mediated ferritinophagy in health and disease, Pharmaceuticals 11 (2018) 114.
- [20] H. Zhao, Y. Lu, J. Zhang, Z. Sun, C. Cheng, Y. Liu, L. Wu, M. Zhang, W. He, S. Hao, K. Li, NCOA4 requires a [3Fe-4S] to sense and maintain the iron homeostasis, J. Biol. Chem. 300 (2024) 105612.
- [21] S. Kuno, K. Iwai, Oxygen modulates iron homeostasis by switching iron sensing of NCOA4, J. Biol. Chem. 299 (2023) 104701.
- [22] A. Nai, M.R. Lidonnici, G. Federico, M. Pettinato, V. Olivari, F. Carrillo, S. Geninatti Crich, G. Ferrari, C. Camaschella, L. Silvestri, F. Carlomagno, NCOA4-mediated ferritinophagy in macrophages is crucial to sustain erythropoiesis in mice, Haematologica 106 (3) (2021) 795–805.
- [23] B.R. Stockwell, J.P. Friedmann Angeli, H. Bayir, A.I. Bush, M. Conrad, S.J. Dixon, S. Fulda, S. Gascón, S.K. Hatzios, V.E. Kagan, K. Noel, X. Jiang, A. Linkermann, M. E. Murphy, M. Overholtzer, A. Oyagi, G.C. Pagnussat, J. Park, Q. Ran, C. S. Rosenfeld, K. Salnikow, D. Tang, F.M. Torti, S.V. Torti, S. Toyokuni, K. A. Woerpel, D.D. Zhang, Ferroptosis: a regulated cell death nexus linking metabolism, redox biology, and disease, Cell 171 (2) (2017) 273–285.

- [24] N. Santana-Codina, A. Gikandi, J.D. Mancias, The role of NCOA4-mediated ferritinophagy in ferroptosis, Adv. Exp. Med. Biol. 1301 (2021) 41–57.
- [25] N. Santana-Codina, M.Q. Del Rey, K.S. Kapner, H. Zhang, A. Gikandi, C. Malcolm, C. Poupault, M. Kuljanin, K.M. John, D.E. Biancur, B. Chen, N.K. Das, K.E. Lowder, C.J. Hennessey, W. Huang, A. Yang, Y.M. Shah, J.A. Nowak, A.J. Aguirre, J. D. Mancias, NCOA4-mediated ferritinophagy is a pancreatic cancer dependency via maintenance of iron bioavailability for iron-sulfur cluster proteins, Cancer Discov. 12 (9) (2022) 2180–2197.
- [26] Y. Fang, X. Chen, Q. Tan, H. Zhou, J. Xu, Q. Gu, Inhibiting ferroptosis through disrupting the NCOA4–FTH1 interaction: a new mechanism of action, ACS Cent. Sci. 7 (6) (2021) 980–9897.
- [27] W.E. Dowdle, B. Nyfeler, J. Nagel, R.A. Elling, S. Liu, E. Triantafellow, S. Menon, Z. Wang, A. Honda, G. Pardee, J. Cantwell, C. Luu, I. Cornella-Taracido, E. Harrington, P. Fekkes, H. Lei, Q. Fang, M.E. Digan, D. Burdick, A.F. Powers, S. B. Helliwell, S. D'Aquin, J. Bastien, H. Wang, D. Wiederschain, J. Kuerth, P. Bergman, D. Schwalb, J. Thomas, S. Ugwonali, F. Harbinski, J. Tallarico, C. J. Wilson, V.E. Myer, J.A. Porter, D.E. Bussiere, P.M. Finan, M.A. Labow, X. Mao, L. G. Hamann, B.D. Manning, R.A. Valdez, T. Nicholson, M. Schirle, M.S. Knapp, E. P. Keaney, L.O. Murphy, Selective VPS34 inhibitor blocks autophagy and uncovers a role for NCOA4 in ferritin degradation and iron homeostasis in vivo, Nat. Cell Biol. 16 (11) (2014) 1069–1079.
- [28] M. Gryzik, A.K. Srivastava, G. Longhi, M. Bertuzzi, A. Gianoncelli, F. Carmona, M. Poli, P. Arosio, Expression and characterization of the ferritin binding domain of nuclear receptor coactivator-4 (NCOA4), Biochim. Biophys. Acta, Gen. Subj. 1861 (11) (2017) 2710–2716.
- [29] A.K. Srivastava, N. Flint, H. Kreckel, M. Gryzik, M. Poli, P. Arosio, F. Bou-Abdallah, Thermodynamic and kinetic studies of the interaction of nuclear receptor coactivator-4 (NCOA4) with human ferritin, Biochemistry 59 (2020) 2707–2717.
- [30] A.K. Srivastava, L.J. Scalcione, P. Arosio, F. Bou-Abdallah, Hyperthermostable recombinant human heteropolymer ferritin derived from a novel plasmid design, Protein Sci. (2022) e4543.
- [31] A.K. Srivastava, M. Poli, P. Arosio, F. Bou-Abdallah, A novel approach for the synthesis of human heteropolymer ferritins of different H to L subunit ratios, J. Mol. Biol. 433 (19) (2021) 167198.

- [32] A.A. Reutovich, A.K. Srivastava, G.L. Smith, A. Foucher, D.M. Yates, E.A. Stach, G. C. Papaefthymiou, P. Arosio, F. Bou-Abdallah, Effect of phosphate and ferritin subunit composition on the kinetics, structure, and reactivity of the iron core in human homo and heteropolymer ferritins, Biochemistry 61 (19) (2022) 2106–2117.
- [33] T. Longo, S. Kim, A.K. Srivastava, L. Hurley, K. Ji, A.J. Viescas, N. Flint, A. Foucher, D.M. Yates, E.A. Stach, G.C. Papaefthymiou, F. Bou-Abdallah, Micromagnetic and morphological characterization of heteropolymer human ferritin cores, Nanoscale Adv. 5 (2023) 208–219.
- [34] G.L. Smith, A.A. Reutovich, A.K. Srivastava, R.E. Reichard, C.H. Welsh, T. Wilkinson, A. Melman, F. Bou-Abdallah, Complexation of ferrous ions by ferrozine, 2,2'-bipyridine and 1,10-phenanthroline: implication for the quantification of iron in biological systems, J. Inorg. Biochem. 220 (2021) 111460.
- [35] G.L. Smith, A.K. Srivastava, A.A. Reutovich, N.J. Hunter, P. Arosio, A. Melman, F. Bou-Abdallah, Iron mobilization from ferritin in yeast cell lysate and physiological implications, Int. J. Mol. Sci. 23 (2022) 6100.
- [36] S.A. Freibert, B.D. Weiler, E. Bill, A.J. Pierik, U. Muhlenhoff, R. Lill, Biochemical reconstitution and spectroscopic analysis of iron–sulfur proteins, Methods Enzymol. 599 (2018) 197–226.
- [37] B. Xia, H. Cheng, V. Bandarian, G.H. Reed, J.L. Markley, Human ferredoxin: overproduction in *Escherichia coli*, reconstitution in vitro, and spectroscopic studies of iron-sulfur cluster ligand cysteine-to-serine mutants, Biochemistry 35 (1996) 9488–9495.
- [38] J.D. Mancias, X. Wang, S.P. Gygi, J.W. Harper, A.C. Kimmelman, Quantitative proteomics identifies NCOA4 as the cargo receptor mediating ferritinophagy, Nature 509 (2014) 105–109.
- [39] S. Kuno, H. Fujita, Y.K. Tanaka, Y. Ogra, K. Iwai, Iron induced NCOA4 condensation regulates ferritin fate and iron homeostasis, EMBO Rep. 23 (2022) e54278.
- [40] F. Hoelzgen, T.T.P. Nguyen, E. Klukin, M. Boumaiza, A.K. Srivastava, E.Y. Kim, R. Zalk, A. Shahar, S. Cohen-Schwartz, E.G. Meyron-Holtz, F. Bou-Abdallah, J. D. Mancias, G.A. Frank, Structural basis for the intracellular regulation of ferritin degradation, Nat. Commun. 15 (2024) 3802.